Risk of decompression sickness in extreme human breath-hold diving.

J.R. FITZ-CLARKE

Department of Physiology and Biophysics, Dalhousie University, 5849 University Avenue Halifax, N.S., Canada B3H 4H7

Fitz-Clarke, JR. Risk of decompression sickness in extreme human breath-hold diving. Undersea Hyperb Med 2009; 36(2):83-91 .The risk of decompression sickness (DCS) in human breath-hold diving is expected to increase as dives progress deeper until a depth is reached where total lung collapse stops additional nitrogen gas uptake. We assembled a database of all documented human breath-hold dives to 100 metres or greater, including both practice and record dives. Between 1976 and 2006 there were 192 such dives confirmed by 24 divers (18 male, 6 female). The deepest dive was to 209 metres. There were two drowning fatalities, and two cases of DCS. Depth-time risk estimates for DCS were derived for single breath-hold dives by modifying probabilistic decompression models calibrated with data from short deep no-stop air dives and submarine escape trials using maximum-likelihood estimation. Arterial nitrogen levels during apnea were adjusted for lung compression and decreased cardiac output. Predicted DCS risk is negligible up to about 100 metres, beyond which risk increases nonlinearly and reaches a plateau around 5 to 7 percent when total lung collapse occurs beyond 230 metres. Results are consistent with data available from deep breath-hold dives.

INTRODUCTION

Competitive breath-hold (BH) divers continue to set new depth records on a single breath of air. Several event categories are recognized within the sport according to the type of equipment used to assist descents and ascents. *Free immersion* (FI) involves pulling oneself down and up a vertical rope using the hands only. *Constant weight* (CW) is the classic free diving discipline using fins alone. *Variable weight* (VW) divers descend on a heavy sled guided by a vertical rope, and swim back to the surface using fins. *No-limits* (NL) is the deepest and most publicized event, where a sled is used for descent and a lift bag inflated at the bottom is used to assist ascent. Total dive times for each category are typically in the range of 3 to 4 minutes for the deepest dives. The present depth record of 214 metres was set by Austrian diver Herbert Nitsch in 2007. Many other highly trained BH divers have reached depths over 100 metres in each discipline (1).

Aside from breath-holding ability, which has surpassed 10 minutes on air at the surface, the physiological factors that might limit the ultimate depth possible by a human diver have not been determined. Decompression sickness (DCS) might become one factor, although it is commonly assumed that dive times are too short and that there is not enough nitrogen available in a single breath of air to cause DCS. Neither of these assumptions can be substantiated. DCS has more commonly been reported after multiple repetitive breath-hold dives when surface intervals between dives are inadequate to eliminate residual nitrogen, but the risk with single deep dives is not clear. In this communication, we report 2 cases of DCS in 192 deep single breath-hold dives.

Experienced BH divers will undoubtedly attempt greater depths and raise the likelihood that serious cases of DCS will occur. Estimation of DCS risk after deep breath-hold dives is

therefore important for logistical planning and to advance insight into human physiology during extreme dives. This paper summarizes BH diving practices beyond 100 metres over a thirty-year period, and derives estimates of DCS risk based on available outcomes incorporated into probabilistic decompression models adapted to single non-repetitive BH dives.

METHODS

We complied a database of all human BH dives conducted to 100 metres or deeper that could be confirmed from reliable sources. Much of the data was available from internet web sites maintained by most champion divers. These sites include detailed training diaries and discussion of daily diving activities leading up to record attempts. Several divers and support personnel were contacted to obtain additional diving data, and reports were accessed from archived magazine articles and biographies describing early deep dives and training routines of retired and deceased divers. We chose a threshold of 100 metres for data collection because information is readily available for deep dives, while dives to shallower depths have been too numerous to document reliably.

Decompression risk analysis was performed using adaptations of three probabilistic models designed for predicting the percent likelihood of DCS on single dives with no prior residual nitrogen. The first is a simple two-compartment parallel mono-exponential model (PME). The other two were developed at the Naval Medical Research Institute (NMRI) (2) and the Defence and Civil Institute for Environmental Medicine (DCIEM) (3). Calibration was carried out independently for this study using DCS outcome data from short deep air exposures in four sources. The first report presents profiles of 299 submarine escape trails from depths up to 187 metres resulting in 4 cases of neurological DCS (4). The second report outlines 58 additional escapes with 2 cases of DCS (5). Descent profiles were either linear or exponential with doubling times included in these reports. Additional data on 88 experimental deep no-stop air dives with bottom times of 8 minutes or less was obtained from two other reports (6,7). These dives produced 4 cases of DCS. The method of maximum likelihood accounts for the dose-response and stochastic nature of decompression sickness (8,9), and was used to find the parameter set for each mathematical model that best matches outcome data within the regime of short deep air dives.

After initial calibration with the 445 open-circuit dives and 10 cases of DCS, each model was adapted to BH diving by incorporating three pragmatic assumptions. (a) Lung perfusion is equal to cardiac output, which is assumed to drop predictably according to an exponentially-decaying function of depth (10) modified by a first-order time constant representing effects of reflex diving bradycardia (11). (b) The rate of arterial nitrogen uptake from the lungs is related to the diffusion-perfusion ratio, with alveolar diffusive surface area obtained as a function of diving depth from a computational model of lung collapse (12). (c) Perfusion of the central nervous system is assumed to remain constant and independent of depth, despite the drop in cardiac output that affects the peripheral circulation. Model equations are presented in the Appendix.

RESULTS

The first diver to reach 100 metres on a single breath of air was Jacques Mayol in 1976. During the subsequent thirty-year period from 1976 to the end of 2006 there were 24 breath-hold divers (18 male, 6 female) who reached depths of 100 metres or greater on a total of

192 dives summarized in Table 1. The deepest diver reached 209 m. Depths of no-limits dives are shown in Figure 1.

Table 1. Breath-Hold Dives to 100 m or Deeper (1976-2006)

Event	Descent	Ascent	Number	Deepest
FI	pull	pull	7	106 m
CW	swim	swim	26	111 m
VW	sled	swim	48	140 m
NL	sled	lift bag	111	209 m
			192	

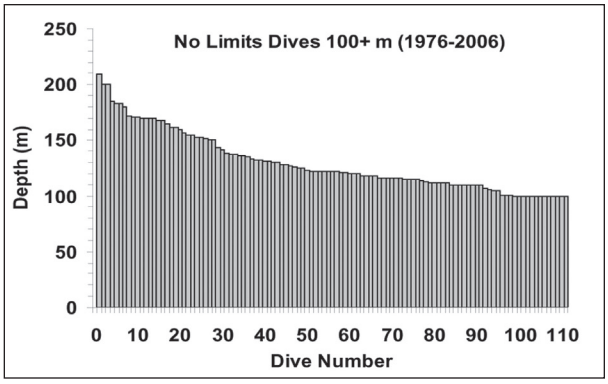

Fig. 1. Depth distribution, deepest to shallowest, of all 111 no-limits dives to 100 metres or greater.

There were two diving fatalities in this data set. The first was a male diver who made a series of progressively deeper no-limits dives in 1995 hoping to establish a world record, but with inadequate safety support. He was last seen drifting away from the rope during ascent from a 128-metre dive, and disappeared. His body was never recovered. The second was a highly experienced female diver who drowned in 2001 when her lift bag failed to inflate at the bottom of a dive to 170 metres. The inflation gas cylinder had not been checked during preparation, and was later found to be empty.

Two divers underwent treatment in a hyperbaric chamber for decompression sickness following single deep breath-hold dives. The first case occurred after a single no-limits dive to 120 metres (13). The second case involved an otherwise successful record-setting dive to 182 metres in the Red Sea. Upon reaching the surface, the male diver experienced severe vertigo and vomited while still in the water. In-water oxygen recompression was attempted for presumed DCS, but the diver quickly became incapacitated, and the effort was aborted. His condition during evacuation progressed to hemiparesis requiring multiple hyperbaric chamber treatments over the next several days with only partial recovery. The total dive time of 5:05 minutes was the longest ever taken for a sled dive. A third individual felt unusually fatigued after a 209-metre record dive, and was also treated with recompression as a precaution, although there were no overt signs of DCS. A recent gastrointestinal illness may have contributed to his weakened state. It should be noted that there have been many more documented cases of DCS associated with repetitive BH dives (14, 15), but these are not considered here. Most BH divers do not conduct repetitive dives on the same day as a deep dive, and usually wait at least 24 hours before diving again.

Risk models were calibrated with depth-time data from air dives and submarine escape exposures shown in Figure 2. Best-fit model parameters and confidence intervals are listed in Table 2. Model predictions in Figure 3 are based on descent and ascent rates of 2 metres per second. Predicted DCS risk is negligible until depth reaches about 100 metres, beyond which it increases nonlinearly. In contrast to open-circuit air diving, we expect BH dive risk to reach a maximum at the depth where alveolar collapse is assumed to be complete. Risk is not expected to increase beyond this depth because nitrogen absorption should stop once the minimum compressed lung volume is reached around 235 metres for a typical initial packed lung volume of 8 litres (12). Maximum DCS risk under these conditions is about 5 to 7 percent, depending on the model. Smaller initial lung volume would reduce this upper bound. Risk drops slightly for deeper dives because

Table 2. Risk Model Parameters Calibrated for Open-Circuit Air Exposures

PME Model:	**T_1**	**T_2**	**A_1**	**A_2**	**LL**
Best Fit	4.63 min	115.6 min	0.00168	0.00784	-57.84745
SE	1.91 min	31.2 min	0.00049	0.00315	
NMRI Model:	**W**	**T_1**	**T_2**	**A**	**LL**
Best Fit	0.937	3.82 min	345.0 min	0.0572	-57.52813
SE	0.004	0.52 min	43.6 min	0.0073	
DCIEM Model:	**A**	**B**	**C**		**LL**
Best Fit	0.00187	83.1	0.001385		-56.78859
SE	0.00102		0.000487		

LL = log-likelihood. SE = standard error. Pressure units are in meters of seawater.

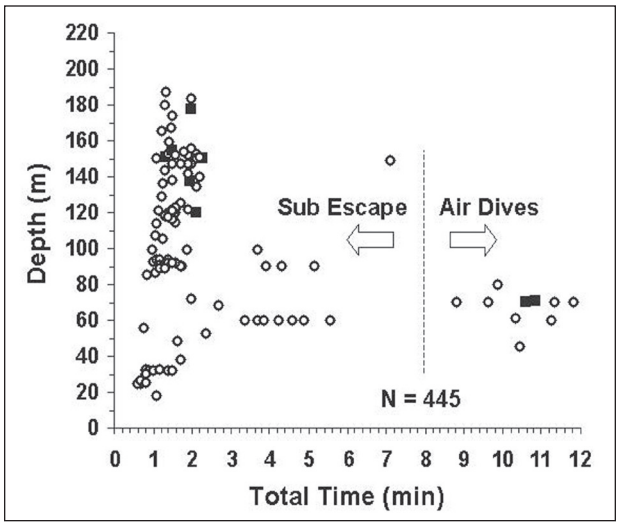

Fig. 2. Submarine escape and no-stop air dive data used for model calibration. Some symbols correspond with multiple man-dives on the same schedule. Black symbols indicate ten cases of DCS.

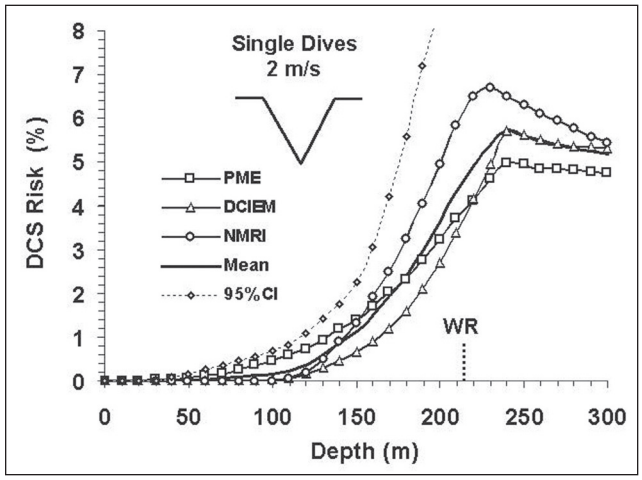

Fig. 3. DCS risk for single breath-hold dives predicted from each model. Mean is shown as thick line. WR = depth of present world record no-limits dive. Plateau and drop in risk is due to lung collapse. Dotted line shows the 95-percent upper confidence interval on mean PDCS.

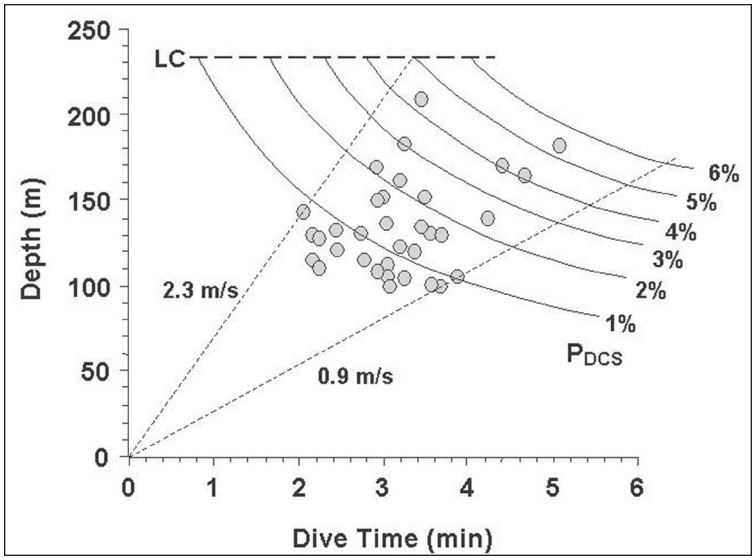

Fig. 4. Predicted DCS risk for breath-hold dives of various depths and total times based on the mean of three models. A subset of BH dives for which times are known is shown as circles. LC indicates depth of lung collapse, beyond which risk does not increase.

longer dive times allow dilution of arterial nitrogen with returning venous blood due to pulmonary shunt after lung collapse. Figure 4 shows the mean prediction of DCS risk from the three models as a function of depth and total dive time. The horizontal line represents lung collapse, beyond which risk does not increase.

DISCUSSION

Several factors have contributed to the steady increase in record depths. Expectation of lung injury due to thoracic squeeze on deep dives turned out not to be substantiated, and this risk is no longer a major consideration. Despite near-total lung collapse on deep dives, re-inflation on ascent is uneventful in most cases as air re-expanding in the large airways overcomes opening pressures in ducts and alveolar sacs. The routine use of mixed-gas scuba allows support divers to maintain great depths safely without contending with nitrogen narcosis. Counter-weight retrieval systems have also been developed to raise the diver quickly in the event of an emergency. Heavier streamlined sleds have led to faster descent velocities with only minimal increases in dive times despite depth advances. Most deep dives reported here had times in the range of 2 to 4 minutes. Only one diver routinely made relatively long dives lasting over 4 minutes.

Although we made every reasonable effort to ensure accuracy and completeness of data collection, there may have been additional BH dives over 100 metres that could not be verified for this study. Several divers stated that they had likely made more practice dives than those reported here, but no record was kept of them. The number of missed dives is likely small, however, considering the extensive logistics and in-water safety support necessary for conducting deep dives.

There have been no previously reported attempts to model DCS risk in BH diving. The pragmatic approach taken here assumes inert gas uptake from the lungs is perfusion-limited (independent of alveolar surface area) at large lung volumes, but gradually decreases and becomes diffusion-limited (dependent on surface area) as depth increases and the lungs approach a collapsed state where gas uptake stops. The depth of human lung collapse has not been directly measured, but was estimated using a model of pulmonary mechanics.

Gas kinetics in BH diving differs from that in open circuit diving and submarine escape due to peripheral circulatory adjustments and changes in alveolar gas levels during apnea (16). Vasoconstriction protects peripheral tissues from nitrogen uptake, while near-normal blood flow is maintained to the brain, hence DCS cases in BH diving almost exclusively involve neurological symptoms. We assume cerebral blood flow remains constant throughout the dive, and the peripheral circulation is non-contributory to DCS. Accordingly, diving reflexes might not protect the diver significantly from neurological DCS. Hypercapnia might increase risk by increasing cerebral blood flow (17, 18), although some protection might be gained by rapid descents compressing molecular skins attached to pre-formed gas micronuclei, increasing their resistance to supersaturation and growth on ascent (19). The affect of very rapid ascents on DCS risk is not known.

Risk models were chosen for their simplicity and the necessity to fit a small number of parameters. More sophisticated risk models based on tissue gas diffusion and bubble dynamics have been used to track risk over repetitive dives (20). The depth-risk relationship for open-circuit dives in this study is similar to that obtained from the model of submarine escape presented by Parker et al. (21) for the case of no prior hyperbaric exposure. Their model, however, predicts a more gradual increase of risk at shallower depths, likely due to different model assumptions and calibration

with a larger less specific data set that included long dives for the purposes of that study.

Parameter confidence intervals in Table 2 are large due to the likelihood surface for each model being relatively flat toward the peak. The level of uncertainty in P_{DCS} predictions is likewise large, due to the small number of DCS cases. The DCIEM model produced the best fit according to the maximum value of LL The bias constant B in this model was fixed at 83.1 msw to maintain consistency with the original model and to prevent the search algorithm from settling on unrealistic negative values. Parameters differed from those in the original models (2, 3) due the data set being more specific for short dives. The most consistent predictions between the three models are within the depth range of calibration data. P_{DCS} curves for dives deeper than 200 metres are model-based extrapolations that assume progressive lung collapse. The BH dive series in Table 1 could not be used for primary calibration because total times were not available for many dives.

The observed incidence of DCS in the BH dives was 2 cases per 192 dives, or 1.0 percent over a large range of depths. The 95 percent binomial confidence interval on the DCS probability for this dive series is 0.3 to 3.7 percent (22, 23). The expected number of DCS cases for this series is the sum of mean probabilities for each of the 192 dives evaluated at their respective depths. This works out to E = 1.09 cases per 192 dives, within the above range. There has been speculation in the diving community that DCS on the dive to 182 metres was precipitated by the unusually long dive time of 5:05 minutes. Figure 4, however, shows that this dive has a predicted risk of 5 percent, as compared with 4 percent for a more typical dive time of 4 minutes. This case of DCS prompted revision of operational guidelines for deep sled diving to include prophylactic post-dive oxygen breathing (24).

DCS risk in BH diving matches that of open circuit diving over much of the depth range because nitrogen gas uptake is not hindered by decreasing alveolar surface area from lung compression until depth exceeds 200 metres. Beyond this depth, arterial nitrogen cannot equilibrate with alveolar nitrogen due to complete pulmonary shunt, and arterial blood becomes increasingly unsaturated as depth increases. This means that existing risk models for air diving might suffice for use in general apnea diving at lesser depths where pulmonary gas exchange remains perfusion-limited, provided that diving reflexes reduce peripheral perfusion while cerebral blood flow remains essentially constant.

It must be emphasized that these predictions have not been independently validated with BH diving data, but are estimates based on the best currently available information. At the present rate of about 6 to 10 BH dives per year being conducted beyond 100 metres, it will take many years to compile enough data to significantly improve risk prediction, particularly at the greatest depths where present data is sparse. In the meantime, it is reasonable to assume that DCS risk approaches 5 to 7 percent on the deepest dives, based on typical descent and ascent rates. While this figure may be acceptable to many deep divers with ready access to emergency recompression, it must be appreciated that DCS cases in BH diving are almost exclusively neurological, and some have been very serious (25). Operational planning must include provision for efficiently managing serious DCS.

APPENDIX

(a) Nitrogen Uptake During Apnea

Arterial nitrogen tension, serving as input to the models during apnea, was calculated using the following equation for whole-lung gas exchange derived from Bohr integration over the capillary length of an alveolar unit (26, 27).

$$P_aN_2 = P_AN_2 - (P_AN_2 - P_vN_2)\exp(-D/\beta Q) \quad (1)$$

Alveolar nitrogen in mm Hg is estimated as $P_AN_2 = 0.79(760)(Z/10 +1)$ where Z is depth in metres. Venous nitrogen tension is assumed to change negligibly during the short dive time due to near-complete tissue uptake, and is fixed at its surface value of $P_vN_2 = 0.79(760) = 600$ mm Hg. Solubility of nitrogen in blood at body temperature is $\beta = (0.017/760)$ mm Hg^{-1}. During BH dives, pulmonary blood flow Q is assumed to decrease with depth from $Q_m = 8.0$ L min^{-1} at the surface to a minimum of $Q_o = 3.0$ L min^{-1} due to diving reflex activation with depth constant $K_{DR} = 0.05$ m^{-1} and time constant $\tau_{DR} = 8$ seconds (10, 11). Alveolar area A_L relative to the surface value A_o is empirically fit to an equation accounting for lung compression (12). Alveolar membrane diffusing capacity for nitrogen D decreases with surface area (28). Capillary membrane diffusing capacity for nitrogen is $D_o = 36$ ml min^{-1} mm Hg^{-1} assuming inflation to total lung capacity at the surface, estimated from values for carbon monoxide (29) corrected for molecular weight and lipid membrane solubility using Graham's law (30). For open-circuit dives, the ratio $D/\beta Q$ is large (over 40), and P_aN_2 is equal to P_AN_2. The resulting equations match open-circuit air DCS risk in the original models, yet yield an asymptotic upper bound of risk when alveoli collapse and $D/\beta Q$ approaches zero during deep BH dives.

$$A_L/A_o = [\,(1+\alpha)(10/(Z+10))^{0.77} - \alpha((Z+10)/10)^{1.2}]$$
$$\alpha = 0.0018 \quad \text{valid for } Z < 235 \text{ m} \quad (2)$$

$$D = D_o\, A_L/A_o \quad (3)$$

$$Q_Z(Z) = Q_o + (Q_m - Q_o)\exp(-K_{DR}\, Z) \quad (4)$$

$$Q(t + \Delta t) = Q(t) + [Q_Z(Z) - Q(t)]\, \Delta t / \tau_{DR} \quad (5)$$

(b) PME Model

The parallel mono-exponential model calculates nitrogen tension in two perfusion-limited compartments following Haldane kinetics (2). Arterial nitrogen $P_aN_2(t)$ is obtained from equation (1). Total risk r(t) is the sum of risks for each compartment, proportional to tissue supersaturation. Parameters to be optimized are A_1, A_2, T_1, and T_2.

$$dP_{Ti}/dt = (P_aN_2 - P_{Ti})/T_i \qquad i = 1,2 \quad (6)$$

$$r_i(t) = A_i(P_{Ti} - P_{amb})/P_{amb} \quad (7)$$

(c) NMRI Model

Nitrogen gas exchange in the NMRI model is calculated by numerically evaluating the convolution integral of the mean residence time function (MRT) over the depth profile (2). The RT describes how long each newly arriving collection of nitrogen molecules remains in the tissue. It has short and long exponential time constants T_1 and T_2, and a weighting term W chosen through parameter optimization. The constant K scales the integrated area to unity. The risk function r(t) is set to zero if negative. This single-tissue model differs from the parallel-compartment Haldane formulation. Parameters to be optimized are W, A, T_1, and T_2.

$$MRT(t) = K\,[W\exp(-t/T_1) - (1 - W)\exp(-t/T_2)] \quad (8)$$

$$P_TN_2 = P_aN_2(t) * MRT(t) = \int_0^\infty P_aN_2(\eta)\; MRT(t - \eta)\, d\eta \quad (9)$$

$$r(t) = A(P_TN_2 - P_{amb}) / P_{amb} \quad (10)$$

(d) DCIEM Model

Nitrogen gas exchange in the DCIEM model is based on nonlinear diffusion between four series-coupled compartments (3). The opening to the first compartment is the arterial nitrogen partial pressure $P_aN_2(t)$. As in the original model, each compartment Pi contains the total tissue gas pressure with a fixed nitrogen fraction of $F_iN_2 = 0.79$. The constant B is fixed at 83.1 msw. Parameters to be optimized are A and C.

$$dP_1/dt = A[(B + P_aN_2 / F_iN_2 + P_1)(P_aN_2 / F_iN_2 - P_1)$$
$$- (B + P_1 + P_2)(P_1 - P_2)] \quad (11a)$$

$$dP_2/dt = A[(B + P_1 + P_2)(P_1 - P_2) - (B + P_2 + P_3)(P_2 - P_3)] \quad (11b)$$

$$dP_3/dt = A[(B + P_2 + P_3)(P_2 - P_3) - (B + P_3 + P_4)(P_3 - P_4)] \quad (11c)$$

$$dP_4/dt = A[(B + P_3 + P_4)(P_3 - P_4)] \quad (11d)$$

$$r_i = C\,(F_iN_2\,P_i - P_{amb})/P_{amb} \qquad i = 1,2,3,4 \quad (12)$$

$$r(t) = r_1 + r_2 + r_3 + r_4 \quad (13)$$

(e) Parameter Optimization

The maximum-likelihood method involves first selecting a risk model and an initial parameter estimate. Each dive profile $Z_i(t)$ is run through the model, and the predicted joint probability of DCS over the entire series of N dives is calculated using observed binary outcome events Y_i as exponents, where $Y_i = 0$ for no DCS and $Y_i = 1$ for DCS. The process is repeated over a suitable range of parameters until the best fit is obtained when the log-likelihood function LL is maximized (least negative). Several widely different initial estimates were provided to ensure that the global maximum was found in the search. Parameter optimization was performed for each model using a converging gradient-search algorithm on an IBM RS6000 computer.

$$P_{DCS} = 1 - \exp\left[-\int_0^{\infty} r(t)\,dt\right] \quad (14)$$

$$L = P^i_{DCS}{}^{Yi}(1 - P^i_{DCS})^{1 - Yi} \quad (15)$$

$$LL = \sum_{i=1}^{N} [Y_i \ln (P^i_{DCS}) + (1-Y_i) \ln (1 - P^i_{DCS})] \quad (16)$$

Standard errors (SE) of parameter estimates are related to the curvature of the LL surface at the peak. Inverting the negative N_P x N_P Fisher information matrix $\mathbf{F_o}$ comprised of second derivatives of LL with respect to each combination of the N_P parameters θ_i gives a symmetric matrix **V** whose diagonal elements are the variances and off-diagonal elements are the covariances (31). SE for each parameter is the square root of its variance. The 95-percent confidence interval for predicted P_{DCS} is $1.96\sigma_o$, where σ_o is obtained by propagation of errors over the N_P independent parameters in the model. **P** is the numerically evaluated local sensitivity vector $\partial P_{DCS}/\partial \theta_i$.

$$\mathbf{F_o} = \left[\frac{\partial^2 L}{\partial \theta_i\, \partial \theta_j}\right] \qquad \mathbf{V} = -\mathbf{F_o}^{-1} \quad (17)$$

$$\sigma_o^2 = \mathbf{P}^T \mathbf{V} \mathbf{P} \quad (18)$$

ACKNOWLEDGMENTS

The author is grateful to the divers who shared personal diving data. Claude Chapuis and Bill Strömberg provided further data and historical information. A complete list of the divers in this series is available by contacting the author.

REFERENCES

1. Association Internationale pour le Développement de l'Apnée (AIDA). www.aida-international.org.
2. Weathersby PK, Survanshi SS, Homer LD, Hart BL, Nishi RY. Statistically-based decompression tables. I. Analysis of standard air dives: 1950-1970 Nav Med Res Inst Report NMRI 85-16, Bethesda. 1985
3. Tikuisis P, Nishi RY, Weathersby PK. Use of the maximum likelihood method in the analysis of chamber air dives. *Undersea Biomed Res* 1988; 15:301-313
4. Donald KW. Submarine escape breathing air: a review and analysis of animal and human experiments by the Royal Navy. *Bull Eur Physiopathol Respir* 1979; 15:739-754
5. Weathersby PK, Survanshi SS, Nishi RY, Thalmann ED. Statistically-based decompression tables. VII. Selection and treatment of primary air and N_2O_2 data. Nav Med Res Inst Report NMRI 92-85. Naval Submarine Medical Research Lab, Groton CT. 1992
6. Nishi RY, Eatock BC, Buckingham IP, Ridgewell BA. Assessment of decompression profiles by ultrasonic monitoring. Phase III: no-decompression dives. DCIEM Report 82-R-38. Department of National Defence, Canada. 1982
7. Spencer MP. Decompression limits for compressed air determined by ultrasonically detected blood bubbles. *J Appl Physiol* 1976; 40:229-235
8. Weathersby PK, Homer LD, Flynn ET. On the likelihood of decompression sickness. *J Appl Physiol* 1984; 57:815-825
9. Homer LD, Weathersby PK. Statistical aspects of the design and testing of decompression tables. *Undersea Biomed Res* 1985; 12:239-249
10. Ferrigno M, Ferretti G, Ellis A, Warkander DE, Costa M, Cerretelli P Lundgren CEG. Cardiovascular changes during deep breath-hold dives in a pressure chamber. *J Appl Physiol* 1997; 83:1282-1290
11. Ferrigno M, Grassi B, Ferretti G, Costa M, Marconi C, Cerretelli P, Lundgren C. Electrocardiogram during deep breath-hold dives by elite divers. *Undersea Biomed Res* 1991; 18:81-91
12. Fitz-Clarke JR. Mechanics of airway and alveolar collapse in human breath-hold diving. *Respir Physiol Neurobiol* 2007; 159:202-210
13. Magno L, Lundgren CEG, Ferrigno M. Neurological problems after breath-hold dives. *Undersea Hyperb Med* 1999; 26 (Suppl.):28-29
14. Schipke JD, Gams E, Kallweit O. Decompression

sickness following breath-hold diving. *Res Sports Med* 2006 14:163-178
15. Paulev P. Decompression sickness following repeated breath-hold dives. *J Appl Physiol* 1965; 20:1028-1031
16. Ferretti G, Costa M, Ferrigno M, Grassi B, Marconi C, Lundgren CE, Cerretelli P. Alveolar gas composition and exchange during deep breath-hold diving and dry breath holds in elite divers. *J Appl Physiol* 1991; 70:794-802
17. Ide K, Eliasziw M, Poulin MJ. Relationship between middle cerebral artery blood velocity and end-tidal PCO_2 in the hypocapnic-hypercapnic range in humans. *J Appl Physiol* 2003; 95: 129–137
18. Palada I, Obad A, Bakovic D, Valic Z, Ivancev V, Dujic Z. Cerebral and peripheral hemodynamics and oxygenation during maximal dry breath-holds. *Respir Physiol Neurobiol* 2007;157:374-381
19. Yount DE. Skins of varying permeability: a stabilization mechanism for gas cavitation nuclei. *J Acoust Soc Am* 1979; 65:1431-1439
20. Gerth WA, Vann RD. Probabilistic gas and bubble dynamics models of decompression sickness occurrence in air and nitrogen-oxygen diving. *Undersea Hyperb Med* 1997; 24:275-292
21. Parker EC, Ball R, Tibbles PM, Weathersby PK. Escape from a disabled submarine: decompression sickness risk estimation. *Aviat Space Environ Med* 2000; 71:109-114
22. Weathersby PK. Uncertainty in decompression safety. In: Schreiner HR, Hamilton RW (Eds). Validation of Decompression Tables. 37th Undersea and Hyperbaric Medical Society Workshop. Bethesda MD. 1987
23. Newcombe RG. Two-sided confidence intervals for the single proportion: comparison of seven methods. *Stat Med* 1998; 17, 857-872
24. Guidelines and Protocol for Sled Diving. Association Internationale pour le Développement de l'Apnée. www.aida-international.org.
25. Kohshi K, Wong RM, Abe H, Katoh T, Abe H, Okudera T, Mano Y. Neurological manifestations in Japanese Ama divers. *Undersea Hyperb Med* 2005; 32:11-20
26. Piiper J, Scheid P. Model for capillary-alveolar equilibration with special reference to O_2 uptake in hypoxia. *Respir Physiol* 1981; 46:193-208
27. Haab P. A model for the study of diffusion and perfusion limitation. *Fed Proc* 1982; 41:2119-2121
28. Stam H, Hrachovina V, Stijnen T, Versprille A. Diffusing capacity dependent on lung volume and age in normal subjects. *J Appl Physiol* 1994; 76:2356-2363
29. Tamhane RM, Johnson RL, Hsia CC. Pulmonary membrane diffusing capacity and capillary blood volume measured during exercise from nitric oxide uptake. *Chest* 2001;120:1850-1856
30. Langø T, Mørland T, Brubakk AO. Diffusion coefficients and solubility coefficients for gases in biological fluids and tissues: a review. *Undersea Hyperb Med* 1996; 23:247-272
31. Nelson W. Applied Life Data Analysis. Wiley and Sons, Inc., New York, 1982.